Loop-to-Loop Pulsed Electromagnetic Signal Transfer Across a Thin Metal Screen With Drude-Type Dispersive Behavior

Martin Štumpf, *Member, IEEE*, and Adrianus T. de Hoop, *Life Member, IEEE*

***Abstract*—A full analytic time-domain analysis is presented for a canonical problem of electromagnetic interference related to the operation of integrated-circuit devices at optical frequencies, where metal screens and substrates can no longer be characterized as perfect electrical conductors, but the plasmonic behavior of conduction electrons in the metal has to be taken into account.**

***Index Terms*—Electromagnetic interference (EMI), modified Cagniard technique, pulsed electromagnetic (EM) field transfer, shielding, time-domain (TD) analysis.**

I. Introduction

With the recent development of high-functionality semiconducting materials, such as indiumphosfide (InP) with promising physical behavior at optical frequencies as components to be implemented in integrated-circuit photonic devices [1], an important electromagnetic interference (EMI) issue presents itself. As a standard practice, in the design of microelectronic devices and systems, the metal screens and substrates in a device are modeled as perfectly conducting constituents. At optical frequencies, however, this is no longer adequate and the plasmonic behavior of the conduction electrons in the metal has to be accounted for in the performance analysis of the system or device and related interconnects. A standard way of developing appropriate design criteria is to study the behavior of canonical (sub)configurations. With this in mind, we investigate the pulsed electromagnetic (EM) signal transfer across a thin, planar, metal sheet, whose electric conduction properties are modeled via the Lorentz theory of electrons, taking into account the collisions of the conduction electrons.

The study can be considered as a contribution to the development of time-domain (TD) definitions of screening effectiveness, as put forward in [2]. To focus on the application of the analysis to microelectronic devices and systems, where the planar topological layout is based on design software with the Kirchhoff circuit loop as the basic constituent, we evaluate the loop-to-loop signal transfer across a planar metal screen. The loops have been modeled via their magnetic dipole equivalents and the dispersion properties of the screen have been accounted for by the Drude model applied to the conduction electrons. The excitation pulse has been taken the (unipolar) power-exponential pulse whose parameters are the pulse amplitude, the pulse rise time, and the pulse time width, all of which comply with the requirements put forward in [2].

The cross-boundary conditions at the metal sheet are modeled via the high-contrast, thin-plate approximation, relating the tangential electric field at the plate to the local value of the volume current density and applying to the tangential magnetic field the condition that it jumps by the amount of the cross-sectional electric current [3].

As is standard practice, the screening effectiveness is defined as the response in the presence of the screen as compared with the one in the absence of the screen. In the case under consideration, the screening effectiveness applies to the magnetic field. The on-axis response is believed to be indicative for the overall properties. The off-axis behavior as well as the electric field transfer (which might be the predominant quantity in circuit boards' interconnects) can be evaluated along similar lines. Illustrative numerical examples are presented for an excitation pulse with parameters that are tailored to address the peculiarities of the physical characteristics of the plasmonic conductivity function and how they influence the pertaining shielding effectiveness.

II. Problem Description

The configuration (see Fig. 1) is excited by a planar pulsed electric current $I^{\mathrm{T}}(t)$ in a transmitting loop $\mathcal{L}^{\mathrm{T}}$ located on one side of, and parallel to, the sheet and the open-circuit induced electric voltage $V^{\mathrm{R}}(t)$ in a receiving loop $\mathcal{L}^{\mathrm{R}}$ located on the other side of the sheet and parallel to it is calculated. Closed-form analytic expressions are obtained for the on-axis response, which leads to an algebraic TD expression for the pertaining transfer impedance

$$V^{\mathrm{R}}(t) = Z(t) \overset{(t)}{*} I^{\mathrm{T}}(t). \tag{1}$$

The position in the problem configuration is specified by the coordinates $\{x, y, z\}$ with respect to the orthogonal Cartesian coordinate system with its origin $\mathcal{O}$ and its basis vec-

Manuscript received July 25, 2017; accepted August 22, 2017. Date of publication October 17, 2017; date of current version January 19, 2018. This work was supported by the Czech Ministry of Education, Youth and Sports under Grant LO1401 of the National Sustainability Program. *(Corresponding author: Martin Štumpf.)*

M. Štumpf is with the SIX Research Centre, Brno University of Technology, Brno 61600, Czech Republic (e-mail: martin.stumpf@centrum.cz).

A. T. de Hoop is H. A. Lorentz Chair Emeritus Professor with the Faculty of Electrical Engineering, Mathematics and Computer Sciences, Delft University of Technology, Delft 2628 CD, The Netherlands (e-mail: a.t.dehoop@tudelft.nl).

Color versions of one or more of the figures in this letter are available online at http://ieeexplore.ieee.org.

Digital Object Identifier 10.1109/TEMC.2017.2754645

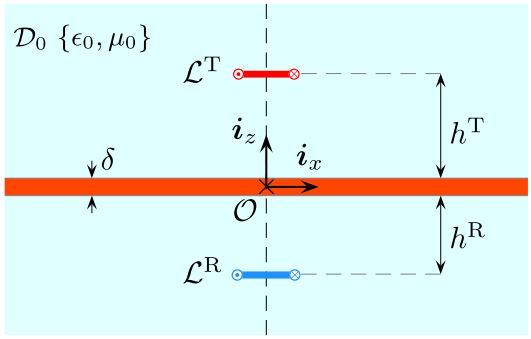

Fig. 1. Plasmonic screen with a transmitting loop $\mathcal{L}^{\mathrm{T}}$ and a receiving loop $\mathcal{L}^{\mathrm{R}}$.

tors $\{\boldsymbol{i}_x, \boldsymbol{i}_y, \boldsymbol{i}_z\}$, respectively. The time coordinate is t and the time-convolution operator is denoted by $\overset{(t)}{*}$.

III. TD Cross-Sheet Boundary Conditions

The EM properties of a metal screen are described via a Drude-type conduction relaxation function [4, Sec. 19.5]

$$\kappa_c(t) = \epsilon_0 \omega_{\mathrm{pe}}^2 \exp(-\nu_c t)\mathrm{H}(t) \tag{2}$$

where $\omega_{\mathrm{pe}} = (n_e \mathrm{e}^2/\epsilon_0 m_{\mathrm{e}})^{1/2}$ is the electron plasma angular frequency, ν_{c} denotes the collision frequency and

1) n_{e} = number density of conduction electrons;
2) $-\mathrm{e}$ = electron charge;
3) m_{e} = electron mass;

and $\mathrm{H}(t)$ is the Heaviside unit step function.

The screen is placed in a homogeneous, isotropic, lossless embedding whose EM behavior is described by its electric permittivity ϵ_0 and magnetic permeability μ_0. The corresponding EM wave speed is $c_0 = (\epsilon_0\mu_0)^{-1/2} > 0$. The thickness of the dispersive layer $\delta > 0$ is assumed to be small with respect to the spatial support of the excitation pulse. The thin screen shows a high contrast with respect to its embedding such that the concept of thin-layer, high-contrast boundary conditions applies [3]. The conditions follow upon applying the volume integrated Maxwell equations to a "pillbox" of vanishing height under the assumption that the layer's TD conductance, viz

$$G^{\mathrm{L}}(t) = \delta\kappa_{\mathrm{c}}(t) \tag{3}$$

is of order $O(1)$ as $\delta \downarrow 0$ for all $t > 0$. Owing to the rotational symmetry of the problem configuration about the z-axis, the cross-boundary conditions are expressed here in the cylindrical coordinates

$$\lim_{z\downarrow 0} E_\phi(r,z,t) - \lim_{z\uparrow 0} E_\phi(r,z,t) \;=\; O(\delta) \text{ as } \delta \downarrow 0 \tag{4}$$

$$\lim_{z\downarrow 0} H_r(r,z,t) - \lim_{z\uparrow 0} H_r(r,z,t) \;=\; G^{\mathrm{L}}(t) \overset{(t)}{*} E_\phi(r,0,t) + O(\delta) \text{ as } \delta \downarrow 0 \tag{5}$$

for all $r = (x^2+y^2)^{1/2} \geq 0$ and $t > 0$, where the subscripts ϕ and r denote the azimuthal and radial components of the EM fields and O denotes the Landau Order symbol [4, p. 1019]. Accounting for the presence of the metal sheet through (2)–(5), the induced voltage is calculated from [5, eq. (33)]

$$V^{\mathrm{R}}(t) \simeq -\mu_0 \mathcal{A}^{\mathrm{R}} \partial_t H_z(0, -h^{\mathrm{R}}, t) \tag{6}$$

where $\mathcal{A}^{\mathrm{R}}$ is the receiving loop's area and $H_z = H_z(r,z,t)$ is the z-component of the radiated magnetic field a closed-form TD expression of which is given in the following sections. The presented methodology is also applicable to expressing the off-axis magnetic field and the electric field.

IV. Transform-Domain Problem Solution

The problem is solved with the aid of a modification of Cagniard's method [6]–[8]. This method combines a one-sided Laplace transformation

$$\hat{H}_z(r,z,s) = \int_{t=0}^{\infty} \exp(-st) H_z(r,z,t)\mathrm{d}t \tag{7}$$

with s as the *real-valued and positive* transformation parameter with the wave-slowness field representation

$$\hat{H}_z(r,z,s) = (s/2\pi)^2 \int_{\alpha=-\infty}^{\infty} \mathrm{d}\alpha \times \int_{\beta=-\infty}^{\infty} \exp[-\mathrm{i}s(\alpha x + \beta y)] \tilde{H}_z(\alpha,\beta,z,s)\mathrm{d}\beta. \tag{8}$$

The transform-domain magnetic field can be expressed as [4, cf. (26.10–15)]

$$\tilde{H}_z = -s\epsilon_0 \tilde{\phi}^K + (s\mu_0)^{-1} \partial_z^2 \tilde{\phi}^K \tag{9}$$

$$\tilde{\phi}^K = s\mu_0 \hat{I}^{\mathrm{T}}(s) \mathcal{A}^{\mathrm{T}} \tilde{G} \tag{10}$$

where $\mathcal{A}^{\mathrm{T}}$ denotes the transmitting loop's area and $\tilde{G} = \tilde{G}(\alpha,\beta,z,s)$ is the (bounded) solution of

$$\partial_z^2 \tilde{G} - s^2 \gamma_0^2(\alpha,\beta)\tilde{G} = 0 \tag{11}$$

where $\gamma_0^2(\alpha,\beta) = c_0^{-2} + \alpha^2 + \beta^2$, subject to the excitation condition

$$\lim_{z\downarrow h^{\mathrm{T}}} \partial_z \tilde{G} - \lim_{z\uparrow h^{\mathrm{T}}} \partial_z \tilde{G} = -1 \tag{12}$$

and the cross-boundary conditions [cf., (4)–(5)]

$$\lim_{z\downarrow 0} \tilde{G} - \lim_{z\uparrow 0} \tilde{G} = 0 \tag{13}$$

$$\lim_{z\downarrow 0} \partial_z \tilde{G} - \lim_{z\uparrow 0} \partial_z \tilde{G} = s\mu_0 \hat{G}^{\mathrm{L}}(s)\tilde{G}|_{z=0}. \tag{14}$$

The corresponding general solution has the form

$$\tilde{G} = \tilde{A}\exp[-s\gamma_0|z - h^{\mathrm{T}}|] + \tilde{A}\tilde{R}\exp[-s\gamma_0(z + h^{\mathrm{T}})] \tag{15}$$

$$\tilde{G} = \tilde{A}\tilde{T}\exp[s\gamma_0(z - h^{\mathrm{T}})] \tag{16}$$

for $z \geq 0$ and $z < 0$, respectively, where

$$\gamma_0(\alpha,\beta) = (c_0^{-2} + \alpha^2 + \beta^2)^{1/2} > 0. \tag{17}$$

Substituting (15)–(16) in (12)–(14), we find

$$\tilde{A} = 1/2s\gamma_0 \tag{18}$$

$$\tilde{T} = \tilde{R} + 1 = 2c_0\gamma_0/[\hat{G}^{\mathrm{L}}(s)/\eta_0 + 2c_0\gamma_0] \tag{19}$$

where $\eta_0 = (\epsilon_0/\mu_0)^{1/2}$ is the free-space admittance. Equations (15)–(19) with (9)–(10) constitute the sought transform-domain solution.

V. TD Problem Solution

Making use of (8)–(10) with (16) and (18)–(19), the on-axis magnetic field can be represented as

$$\hat{H}_z(0,-h^{\mathrm{R}},s) = \frac{s^3 c_0 \hat{I}^{\mathrm{T}}(s)\mathcal{A}^{\mathrm{T}}}{4\pi^2}\int_{\alpha=-\infty}^{\infty}\mathrm{d}\alpha \times \int_{\beta=-\infty}^{\infty}\frac{\alpha^2+\beta^2}{\hat{G}^{\mathrm{L}}(s)/\eta_0 + 2c_0\gamma_0}\exp[-s\gamma_0(h^{\mathrm{T}}+h^{\mathrm{R}})]\mathrm{d}\beta. \tag{20}$$

Upon introducing

$$\{\alpha,\beta\} = \{\sigma\cos(\psi), \sigma\sin(\psi)\} \tag{21}$$

with $\sigma \geq 0$ and $\{0 \leq \psi < 2\pi\}$, (20) is rewritten as

$$\hat{H}_z(0,-h^{\mathrm{R}},s) = [s^3 c_0 \hat{I}^{\mathrm{T}}(s)\mathcal{A}^{\mathrm{T}}/2\pi] \times \int_{\sigma=-\infty}^{\infty}\frac{\sigma^3}{\hat{G}^{\mathrm{L}}(s)/\eta_0 + 2c_0\bar{\gamma}_0}\exp[-s\bar{\gamma}_0(h^{\mathrm{T}}+h^{\mathrm{R}})]\mathrm{d}\sigma \tag{22}$$

where $\bar{\gamma}_0 = \bar{\gamma}_0(\sigma)$ is given by

$$\bar{\gamma_0} = (c_0^{-2}+\sigma^2)^{1/2} > 0. \tag{23}$$

The TD counterpart is found through the substitution

$$\bar{\gamma}_0(\sigma)(h^{\mathrm{T}}+h^{\mathrm{R}}) = \tau \tag{24}$$

for $\{\tau \in \mathbb{R}; \tau > 0\}$ that allows us to cast (22) into the following form:

$$\hat{H}_z(0,-h^{\mathrm{R}},s) = \left[s^3 c_0 \hat{I}^{\mathrm{T}}(s)\mathcal{A}^{\mathrm{T}}/2\pi(h^{\mathrm{T}}+h^{\mathrm{R}})^4\right] \times \int_{\tau=T}^{\infty}\exp(-s\tau)\frac{\tau(\tau^2-T^2)}{\hat{G}^{\mathrm{L}}(s)/\eta_0 + 2\tau/T}\mathrm{d}\tau \tag{25}$$

where $T = (h^{\mathrm{T}}+h^{\mathrm{R}})/c_0$ denotes the travel time of the pulse. By the application of some elementary rules of the one-sided time Laplace transformation (see [9, (29.2.5), (29.2.15), and (29.3.8)]), combined with Lerch's theorem on the uniqueness of the transformation at real, positive, transform parameter we finally obtain

$$V^{\mathrm{R}}(t) = -\frac{\mathcal{A}^{\mathrm{T}}\mathcal{A}^{\mathrm{R}}}{(h^{\mathrm{T}}+h^{\mathrm{R}})^4}\frac{\partial_t^4 I^{\mathrm{T}}(t)}{2\pi\eta_0} \overset{(t)}{*} \left\{\frac{T(t^2-T^2)}{2}\mathrm{H}(t-T) - \Omega_0\int_{\tau=T}^{t}\frac{\tau(\tau^2-T^2)}{4\tau^2/T^2}\exp[-(T/2\tau)\Omega_0(t-\tau)] \times \exp[-\nu_{\mathrm{c}}(t-\tau)]\mathrm{d}\tau\right\} \tag{26}$$

with $\Omega_0 = \delta\omega_{\mathrm{pe}}^2/c_0$, which is the main result of this letter. The first contribution in (26), say V_0^{R}, represents the induced voltage in absence of the shielding metal screen and can be rewritten as

$$V_0^{\mathrm{R}}(t) = -\mu_0\mathcal{A}^{\mathrm{T}}\mathcal{A}^{\mathrm{R}}\left\{\partial_t I^{\mathrm{T}}(t-T)/\left[2\pi(h^{\mathrm{T}}+h^{\mathrm{R}})^3\right] + \partial_t^2 I^{\mathrm{T}}(t-T)/\left[2\pi c_0(h^{\mathrm{T}}+h^{\mathrm{R}})^2\right]\right\} \tag{27}$$

which is fully compatible with the results given in [5, Sec. IX]. It is interesting to note in this respect that the voltage response in (27) is composed of the near- and intermediate-field constituents only [4, Sec. 26.4]. Sufficiently behind the wavefront where the effect of the plasmonic conductivity becomes effective, the decomposition of the field response into its near-, intermediate-, and far-field constituents is no longer straightforward.

VI. TD Solution for an Instantaneously-Reacting Metal Screen

The static conductivity σ_{c} leads to the conduction relaxation function

$$\kappa_{\mathrm{c}}(t) = \sigma_{\mathrm{c}}\delta(t) \tag{28}$$

the induced voltage follows from (6) and the corresponding TD counterpart of (25) relying on Lerch's uniqueness theorem of the one-sided Laplace transformation [10, pp. 63–65]. This way leads to

$$V^{\mathrm{R}}(t) = -\frac{\mathcal{A}^{\mathrm{T}}\mathcal{A}^{\mathrm{R}}}{(h^{\mathrm{T}}+h^{\mathrm{R}})^4}\frac{\partial_t^4 I^{\mathrm{T}}(t)}{2\pi\eta_0} \overset{(t)}{*} \frac{t(t^2-T^2)}{G^{\mathrm{L}}/\eta_0 + 2t/T}\mathrm{H}(t-T) \tag{29}$$

where $G^{\mathrm{L}} = \delta\sigma_{\mathrm{c}}$. The instantaneously reacting conductive screen has been previously analyzed in [11] using a Fourier integral based modification of Cagniard's method [12, Sec. 4.2].

VII. Illustrative Numerical Results

The exciting electric-current pulse is taken to be the (unipolar) power-exponential pulse [13]

$$I^{\mathrm{T}}(t) = I_{\mathrm{m}}^{\mathrm{T}}(t/t_{\mathrm{r}})^n\exp[-n(t/t_{\mathrm{r}}-1)]\mathrm{H}(t) \tag{30}$$

that is characterized by its

1) $I_{\mathrm{m}}^{\mathrm{T}}$ = pulse amplitude;
2) t_{r} = pulse rise time;
3) t_{w} = pulse time width; and
4) n = pulse rising power.

The time Laplace transformation of the excitation pulse reads

$$\hat{I}^{\mathrm{T}}(s) = I_{\mathrm{m}}^{\mathrm{T}}\,t_{\mathrm{r}}^{-n}(s+n/t_{\mathrm{r}})^{-n-1}\Gamma(n+1)\exp(n) \tag{31}$$

where $\Gamma(x)$ denotes the Euler Gamma function. The pulse time width is related to t_{r} and n via $t_{\mathrm{w}} = t_{\mathrm{r}}\,n^{-n-1}\Gamma(n+1)\exp(n)$.

For validation purposes, we shall next evaluate the on-axis shielding effectiveness that is defined as [4, p. 975]

$$S\mathrm{dB} = 20\log_{10}|\hat{Z}_0(\mathrm{i}\omega)/\hat{Z}(\mathrm{i}\omega)| \tag{32}$$

where ω is the real-valued and positive angular frequency and $\hat{Z}_0$ denotes the transfer impedance for the configuration without the screen. This impedance follows from the real-FD counterpart of (27) as

$$\hat{Z}_0(\mathrm{i}\omega) = \frac{\omega\mu_0\mathcal{A}^{\mathrm{T}}\mathcal{A}^{\mathrm{R}}}{2\pi(h^{\mathrm{T}}+h^{\mathrm{R}})^3}(\omega T - \mathrm{i})\exp(-\mathrm{i}\omega T). \tag{33}$$

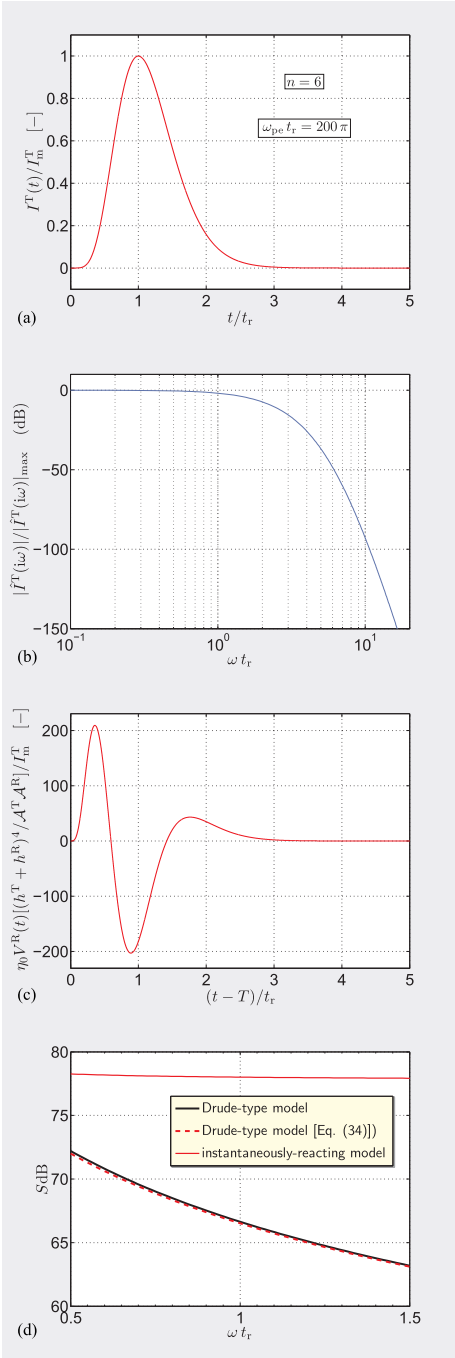

Fig. 2. Excitation electric-current pulse with its (a) pulse shape and (b) amplitude spectral diagram; (c) (normalized) induced voltage pulse behind the metal screen; and (d) resulting shielding effectiveness as calculated via the FFT of the voltage signals and using the approximate formula (34).

In view of (1) and (6), the thus defined shielding effectiveness can also be written as the ratio of the magnetic-field strength at the position of the receiving loop before and after placement of the screen. Accordingly, we can validate the results with the help of the approximate formula [14, (10.15b)]

$$S\mathrm{dB} \simeq 20\log_{10}[|\hat{\kappa}_{\rm c}(\mathrm{i}\omega)|\delta/2\eta_0] \tag{34}$$

where we have substituted the FD counterpart of the conduction relaxation function (see the appendix).

In the example that follows, we take $\hbar\omega_{\rm pe} = 8.55\,\mathrm{eV}$, $\hbar\nu_{\rm c} = 0.0184\,\mathrm{eV}$ describing the properties of gold [15]. The radius of the both transmitting and receiving loops is 0.001 mm and $h^{\rm T} = h^{\rm R} = 0.10$ mm. The thickness of the screen is taken as $\delta = 0.001$ mm (see Fig. 1). The excitation pulse is described with $I^{\rm T}_{\rm m} = 1.0$ (A), $n = 6$, and $\omega_{\rm pe} t_{\rm r} = 200\,\pi$. For the chosen parameters, $\delta/c_0 t_{\rm w} \simeq 0.067$ and the absolute value of the layer's admittance at the "pulse corner frequency" [see eq. (31)] are $|\hat{Y}^{\rm L}(\mathrm{i}n/t_{\rm r})| \simeq 11.75$ S, thus meeting the necessary conditions for the cross-boundary conditions to apply (see the appendix). Figures 2(a) and 2(b) show the excitation pulse shape with the corresponding amplitude spectral (Bode) diagram, respectively. The pulse shape of the voltage induced behind the metallic screen in given in Fig. 2(c) and the corresponding (frequency-dependent) shielding effectiveness as calculated with the aid of both the FFT of (26) and (27) and the approximate formula (34) is shown in Fig. 2(d). Good agreement throughout the chosen frequency range validates the results.

The shielding effectiveness has been further calculated via the FFT of (27) and (29) concerning the relaxation-free conduction model according to Section VI with the conductivity of gold $\sigma_{\rm c} = 41 \cdot 10^6$ S/m taken from [14, Tab. 10.2]. This implies the layer's (frequency-independent) conductance $G^{\rm L} = 41.0$ S. The resulting shielding effectiveness is then about 78 dB over the frequency range of interest [see Fig. 2(d)], which is in agreement with the approximate formula since $20\log_{10}(\sigma_{\rm c}\delta/2\eta_0) \simeq 77.8$ dB. The latter is in accordance with the assumption from Section VI valid at low frequencies. At high frequencies, the classic plane-wave shielding model predicts that SdB increases with $\delta\omega^{1/2}$ due to the absorption as the wave traverses the layer [16, Sec. 10.1]. As long as the thin-sheet, high-contrast boundary conditions apply, multiple reflections in the layer are not distinguishable and the shielding efficiency drop as seen in Fig. 2(d) can be largely attributed to the conduction relaxation effects.

VIII. Conclusion

The configuration that has been investigated can serve as a canonical model in the course of developing a general pulsed-field TD characterization of the screening effectiveness of a thin metal screen, as put forward in [2]. In this respect, it is mentioned that the modified Cagniard technique can also provide TD expressions for the stored energies in the electric and magnetic field (as proposed in [2]).

Appendix
Layer's Conductance/Admittance Relaxation Function

In the description of the conduction properties of a metal, the Lorentz model is used as a standard, where the inertia and collision properties of the conduction electrons are taken into account. The Drude-model only accounts for the effect of collisions and neglects the inertia of the conduction electrons. In the frequency-domain (FD) description, this means that the signal frequency of operation is to be a certain amount below the electron plasma frequency. Using the time Laplace transformation of (3) with (2), we get

$$\hat{G}^{\rm L}(s) = \delta\epsilon_0\omega_{\rm pe}^2/(s+\nu_{\rm c}). \tag{35}$$

The corresponding FD admittance of the layer is

$$\hat{Y}^{\rm L}(\mathrm{i}\omega) = \frac{\delta\epsilon_0\omega_{\rm pe}^2/\nu_{\rm c}}{1+\omega^2/\nu_{\rm c}^2} - \mathrm{i}\frac{\delta\epsilon_0\omega_{\rm pe}^2\omega/\nu_{\rm c}^2}{1+\omega^2/\nu_{\rm c}^2} \tag{36}$$

where ω being the real-valued and positive angular frequency. In case the collision effects can be neglected, the FD layer's admittance is purely inductive

$$\hat{Y}^{\mathrm{L}}(\mathrm{i}\omega)|_{\nu_{\mathrm{c}}\downarrow 0} \;=\; -\,\mathrm{i}\delta\epsilon_0\omega_{\mathrm{pe}}^2/\omega. \tag{37}$$

Obviously, the cross-boundary conditions apply if the electron plasma frequency is large enough with respect to the frequency of operation. For typical plasmonic materials, such as gold and silver whose plasmonic angular frequency is of order of 10^{16} rad/s, the maximum operating signal frequency for the sheet of thickness $\delta = 10^{-6}$ m is in the range of tens of terahertz.

ACKNOWLEDGMENT

The authors want to express their gratitude to the (anonymous) reviewers of the manuscript. Their constructive comments have been incorporated in the present version and have led to a number of improvements.

REFERENCES

[1] A. S. Francomacaro, D. K. Wickenden, and S. J. Lehtonen, "Microelectronic substrates for optoelectronic packages," *Johns Hopkins APL Tech. Dig.*, vol. 28, no. 1, pp. 40–46, 2008.

[2] R. Araneo and S. Celozzi, "Toward a definition of the shielding effectiveness in the time-domain," in *Proc. 2013 IEEE Int. Symp. Electromagn. Compat.*, 2013, pp. 113–117.

[3] A. T. de Hoop and L. Jiang, "Pulsed EM field response of a thin, high-contrast, finely layered structure with dielectric and conductive properties," *IEEE Trans. Antennas Propag.*, vol. 57, no. 8, pp. 2260–2269, Aug. 2009.

[4] A. T. de Hoop, *Handbook of Radiation and Scattering of Waves*. London, UK: Academic Press (freely downloadable, for private use, from www.atdehoop.com).

[5] A. T. de Hoop, I. E. Lager, and V. Tomassetti, "The pulsed-field multiport antenna system reciprocity relation and its applications—A time-domain approach," *IEEE Trans. Antennas Propag.*, vol. 57, no. 3, pp. 594–605, Mar. 2009.

[6] L. Cagniard, *Réflexion et réfraction des ondes séismiques progressives*. Paris, France: Gauthier-Villars, 1939.

[7] L. Cagniard, *Reflection and Refraction of Progressive Seismic Waves*. New York, NY, USA: McGraw-Hill, 1962 (Translation by Flinn, E., Dix, C. H. of Réflexion et réfraction des ondes séismiques progressives, Paris, Gauthier-Villars, 1939).

[8] A. T. de Hoop, "A modification of Cagniard's method for solving seismic pulse problems," *Appl. Scientific Res.* B, vol. 8, pp. 349–356, 1960.

[9] M. Abramowitz and I. A. Stegun, *Handbook of Mathematical Functions*. New York, NY, USA: Dover, 1972.

[10] D. V. Widder, *The Laplace Transform*. Princeton, NJ, USA: Princeton Univ. Press, 1946.

[11] P. Burghignoli, G. Lovat, R. Araneo, and S. Celozzi, "Time-domain shielding of a thin conductive sheet in the presence of pulsed vertical dipoles," *IEEE Trans. Electromagn. Compat.*, 10.1109/TEMC.2017.2702560.

[12] W. C. Chew, *Waves and Fields in Inhomogeneous Media*. Piscataway, NJ, USA: IEEE Press, 1995.

[13] A. T. de Hoop and I. E. Lager, "Pulsed fields EM interference analysis in digital signal wireless interconnects," in *Proc. 41st Eur. Microw. Conf.*, 2011, pp. 313–316.

[14] F. M. Tesche, M. V. Ianoz, and T. Karlsson, *EMC Analysis Methods and Computational Models*. Hoboken, NJ, USA: Wiley, 1997.

[15] M. G. Blaber, M. D. Arnold, and M. J. Ford, "Search for the ideal plasmonic nanoshell: The effects of surface scattering and alternatives to gold and silver," *J. Phys. Chem. C*, vol. 113, pp. 3041–3045, 2009.

[16] C. R. Paul, *Introduction to Electromagnetic Compatibility*, 2nd ed. Hoboken, NJ, USA: Wiley, 2006.

Martin Štumpf (M'14) was born in Ćàslav, The Czech Republic, on September 22, 1983. He received the B.Sc., M.Sc., and Ph.D. degrees from the Brno University of Technology (BUT), Brno, The Czech Republic, in 2006, 2008, and 2011, respectively.

After defending the Ph.D., he spent a year and a half as a Postdoctoral Fellow at the ESAT-TELEMIC division, Katholieke Universiteit Leuven, Leuven, Belgium (2011–2012). He is currently is an Associate Professor at SIX Research Centre, BUT. He also spent several months as a Visiting Scientist at Otto-von-Guericke University, Magdeburg, Germany (2008) and at Delft University of Technology, Delft, The Netherlands (2009–2010 and 2014). His main research interests include mathematical modeling of electromagnetic and acoustic wave and diffusive phenomena.

Dr. Štumpf received a Young Scientist Best Paper Award (3rd prize) and a Young Scientist Award at the URSI International Symposium on Electromagnetic Theory in Hiroshima, Japan (2013), a Young Scientist Award at the URSI International Symposium on Electromagnetic Theory in Berlin, Germany (2010), a Radioengineering Young Scientist Award at the Radioelektronika conference (2011), and the Best Diploma Thesis Award from the MTT/AP/ED/EMC joint Chapter of the Czechoslovak Section of IEEE (2008).

Adrianus T. de Hoop (M'00) was born in Rotterdam, The Netherlands, on December 24, 1927. He received the M.Sc. degree in electrical engineering and the Ph.D. degree in the technological sciences from the Delft University of Technology, Delft, The Netherlands, in 1950 and 1958, respectively, both with the highest distinction.

He was with Delft University of Technology as an Assistant Professor from 1950 to 1957, Associate Professor from 1957 to 1960, and Full Professor of electromagnetic theory and applied mathematics from 1960 to 1996. Since 1996, he has been Lorentz Chair Emeritus Professor in the Faculty of Electrical Engineering, Mathematics and Computer Sciences of this University. In 1970, he founded the Laboratory of Electromagnetic Research, which has developed into a world-class center for electromagnetics, having a huge impact on the worlds electromagnetic community and on electromagnetic research and education in the Netherlands. His research interests are in the broad area of wave field modeling in acoustics, electromagnetics, and elastodynamics. His interdisciplinary insights and methods in this field can be found in his seminal *Handbook of Radiation and Scattering of Waves* (Academic, 1995, xxx + 1083 pp.), with wave field reciprocity serving as one of the unifying principles governing direct and inverse scattering problems and wave propagation in complex (anisotropic and dispersive) media. He spent a year (1956–1957) as a Research Assistant with the Institute of Geophysics, University of California at Los Angeles, CA, USA, where he pioneered a modification of the Cagniard technique for calculating impulsive wave propagation in layered media, later to be known as the "Cagniard-DeHoop technique." This technique is presently considered as a benchmark tool in analyzing time-domain wave propagation. During a sabbatical leave at Philips Research Laboratories, Eindhoven, The Netherlands (1976–1977), he was involved in research on magnetic recording theory. Since 1982, he has been, on a regular basis, Visiting Scientist with Schlumberger-Doll Research, Ridgefield, CT, USA (presently at Cambridge, MA, USA), where he contributes to research on geophysical applications of acoustic, electromagnetic, and elastodynamic waves.

Dr. De Hoop is currently working on a monograph with the title "Wavefield Physics–An arraystructured theory." How such a theory works out for electromagnetic fields can be found in the invited paper for the Centennial Issue of PROCEEDINGS OF THE IEEE, 101, 2013, pp. 434–450 (open-source publication). He received the 1989 Research Medal of the Royal Institute of Engineers in The Netherlands, the IEEE 2001 Heinrich Hertz Gold Research Medal, and the 2002 URSI (International Scientific Radio Union) Balthasar van der Pol Gold Research Medal. In 2003, H. M. the Queen of The Netherlands appointed him "Knight in the Order of the Netherlands Lion." He is a Member of the Royal Netherlands Academy of Arts and Sciences and a Foreign Member of the Royal Flemish Academy of Belgium for Science and Arts. He holds an Honorary Doctorate in the Applied Sciences from Ghent University, Belgium (1981) and an Honorary Doctorate (2008) in the Mathematical, Physical and Engineering Sciences from Växjö University (since 2010, Linnaeus University), Växjö, Sweden. Grants from the "Stichting Fund for Science, Technology and Research" (founded by Schlumberger Limited) supported his research at the Delft University of Technology.